Analytical and Bioanalytical Chemistry
https://doi.org/10.1007/s00216-019-02075-8

RESEARCH PAPER

Novel probes for label-free detection of neurodegenerative GGGGCC repeats associated with amyotrophic lateral sclerosis

Motahareh Taki[1] · Kushal J. Rohilla[2] · Maria Barton[2] · Madison Funneman[1] · Najiyah Benzabeh[1] · Swati Naphade[3] · Lisa M. Ellerby[3] · Keith T. Gagnon[1,2] · Mohtashim H. Shamsi[1]

Received: 30 May 2019 / Revised: 18 July 2019 / Accepted: 6 August 2019

Abstract

DNA repeat expansion sequences cause a myriad of neurological diseases when they expand beyond a critical threshold. Previous electrochemical approaches focused on the detection of trinucleotide repeats (CAG, CGG, and GAA) and relied on labeling of the probe and/or target strands or enzyme-linked assays. However, detection of expanded GC-rich sequences is challenging because they are prone to forming secondary structures such as cruciforms and quadruplexes. Here, we present label-free detection of hexanucleotide GGGGCC repeat sequences, which cause the leading genetic form of frontotemporal dementia (FTD) and amyotrophic lateral sclerosis (ALS). The approach relies on capturing targets by surface-bound oligonucleotide probes with a different number of complementary repeats, which proportionately translates the length of the target strands into charge transfer resistance (R_{CT}) signal measured by electrochemical impedance spectroscopy. The probe carrying three tandem repeats transduces the number of repeats into R_{CT} with a 3× higher calibration sensitivity and detection limit. Chronocoulometric measurements show a decrease in surface density with increasing repeat length, which is opposite of the impedance trend. This implies that the length of the target itself can contribute to amplification of the impedance signal independent of the surface density. Moreover, the probe can distinguish between a control and patient sequences while remaining insensitive to non-specific Huntington's disease (CAG) repeats in the presence of a complementary target. This label-free strategy might be applied to detect the length of other neurodegenerative repeat sequences using short probes with a few complementary repeats.

Keywords Nucleic acid biosensing · Electrochemical biosensors · Repeat expansion disorders · Amyotrophic lateral sclerosis · Electrochemical impedance spectroscopy

Introduction

DNA microsatellite sequences comprise small repeating units of 2–6 nucleotides that occur naturally in 30% of the human genome [1, 2]. Repeat sequences play a crucial role in genome function and evolution; however, their expansion beyond a certain threshold of repeating units is associated with over 30 neurological and neuromuscular diseases [3]. The leading genetic form of frontotemporal dementia (FTD) and amyotrophic lateral sclerosis (ALS) is caused by the expansion of a GGGGCC/CCCCGG hexanucleotide repeat in the first intron of Chromosome 9 Open Reading Frame 72 (*C9ORF72*) gene [4, 5].

Current testing for most genetic repeat expansion diseases involves state-of-the-art DNA microarray technology that relies on fluorescence labels and repeat-primed PCR for signal amplification [6]. Although DNA microarrays have significantly reduced the time delay and cost of testing, they have critical limitations for the detection of disease-associated hexanucleotide repeat sequences because they are typically GC-rich [7–9], and polymerases do not traverse efficiently through highly repetitive and GC-rich sequences [10, 11]. Moreover, large repeat expansions do not resolve well by

Electronic supplementary material The online version of this article (https://doi.org/10.1007/s00216-019-02075-8) contains supplementary material, which is available to authorized users.

✉ Mohtashim H. Shamsi
mshamsi@siu.edu

[1] Department of Chemistry & Biochemistry, Southern Illinois University, 1245 Lincoln Dr, Carbondale, IL 62901, USA

[2] Biochemistry and Molecular Biology, Southern Illinois University School of Medicine, Carbondale, IL 62901, USA

[3] The Buck Institute for Research on Aging, 8001 Redwood Blvd, Novato, CA 94945, USA

Published online: 21 August 2019

gel-electrophoresis [12]. On the other hand, high-throughput whole-genome sequencing technologies are currently limited to ~ 150 base pair read lengths [13]. The most widely used method to detect *C9ORF72* repeat expansions is repeat-primed PCR (RP-PCR) with fragment length analysis [14], where the interpretation is usually challenging due to indels in the flanking regions of the repeat, which is prone to both false positives and false negatives [14]. Another limitation is that these PCR techniques do not provide an estimate of the length of the repeat expansions. While used as a gold standard, Southern blotting requires a significant amount of input DNA (≥ 10 μg) and size estimates may be imprecise due to somatic heterogeneity [14, 15]. These limitations present challenges for genetic testing laboratories [16]. Nevertheless, a rapid and sensitive detection method which requires low amounts of patient DNA or RNA input may potentially facilitate diagnosis and timely treatment of such patients [17, 18].

Electrochemical biosensing approaches are attractive because they offer simple operation, rapid response, high sensitivity, inexpensive implementation, and the ability to miniaturize for point-of-care diagnostics [19]. Challenges in the current detection methods of repeat sequences may be resolved by electrochemical methods due to high sensitivity of up to pg/μL range [20]. To date, detection of repeat expansion involving electrochemical approach has been limited to detect trinucleotide repeats (CGG, CAG, and GAA) [20–29]. To capture target, these studies either involved surface-bound small molecules for recognition or very large DNA probe sequences (> 100-mer) with covalently bound labels [20, 26, 27, 29]. For signal amplification, these methods relied heavily on multiple hybridization steps and several reporter probes [21–23], PCR amplification [29], enzyme-linked steps [27], and electroactive labels [20, 26]. However, for real-world applications, simple methods with minimal steps are desirable.

In this work, we present a simple label-free approach that detects the length of higher order 100% GC-content (i.e., hexanucleotide GGGGCC repeats) single-stranded DNA and RNA sequences. Such sequences are challenging due to their ability to make complicated secondary structures and do not resolve well by techniques like electrophoresis [12]. Scheme 1 illustrates the label-free detection strategy for GGGGCC repeats that relies on the number of complementary repeat units present in the surface-bound 18-mer long DNA probes that are used. Hybridization between the DNA/RNA targets with increasing repeat length using probes with single repeat (P1) or three tandem repeats (P2) were studied without any signal amplification strategy through various electrochemical techniques. Chronocoulometry (CC) was used to estimate the surface densities of the hybrid duplexes formed by the probes (P1 and P2) and DNA targets. Electrochemical impedance spectroscopy (EIS) was used to measure the charge transfer resistance (R_{CT}) posed by the immobilization of the DNA and RNA targets on P1-/P2-modified electrodes. In addition, cyclic voltammetry measured the change in overpotential with respect to repeat lengths.

Experimental

Reagents and materials

$K_4[Fe(CN)_6]$, $K_3[Fe(CN)_6]$ and sulfuric acid (98%) were purchased from Thermo Fisher Scientific (Waltham, MA). Tris(hydroxymethyl)aminomethane (Tris-ClO_4), $Ru(NH_3)_6Cl_3$, 6-Mercapto-1-hexanol (MCH) and 10× phosphate buffered saline (100 mM phosphate and 1.54 M sodium chloride) were purchased from Sigma-Aldrich (St. Louis, MO). Gold disc electrodes and platinum wire electrodes were purchased from CH Instruments (Bee Cave, TX). The Ag/AgCl reference electrodes and velvet cloth for polishing electrodes were obtained from Bioanalytical Systems Inc. (West Lafayette, IN). The HPLC purified probe sequences with a 6-hydroxyhexyl disulfide group at the 5′ end (P1 and P2) and the complementary sequences (C1, C3 and C6) were purchased from IDT (Integrated DNA Technologies, Coralville, IA). Table 1 shows the DNA probe sequences (P1 and P2) carrying one and three CCCCGG capture repeats, respectively. The DNA target sequences C1, C3, and C6 contain one, three, and six complementary GGGGCC repeats, respectively. Purified GGGGCC repeat-containing RNA targets with 4–16 repeats were used in this study and in vitro transcribed from DNA templates purchased from IDT (Table S1). In vitro transcription and gel-purification of repeat RNA was performed by standard methods as previously described [30], and concentration was determined by spectrophotometry (absorbance at 260 nm) using Beer's law and calculated extinction coefficients (https://www.atdbio.com/tools/oligo-calculator) (single-stranded RNA nearest-neighbor model).

Preparation of RNA samples

The RNA containing Huntington's disease (HD) repeats were prepared from an isogenic HD iPSC stem cell model with 72 units of CAG trinucleotide repeats as described [31]. RNA was purified from neural stem cell cultured samples. Patient-derived induced pluripotent stem cells (iPSCs) with less than 30 GGGGCC repeat expansion and with approximately 450 GGGGCC repeat expansion were obtained from Cedars Sinai iPSC Core facility. iPSCs were grown in flasks precoated with GeltrexTM matrix (ThermoFisher Scientific) in the presence of

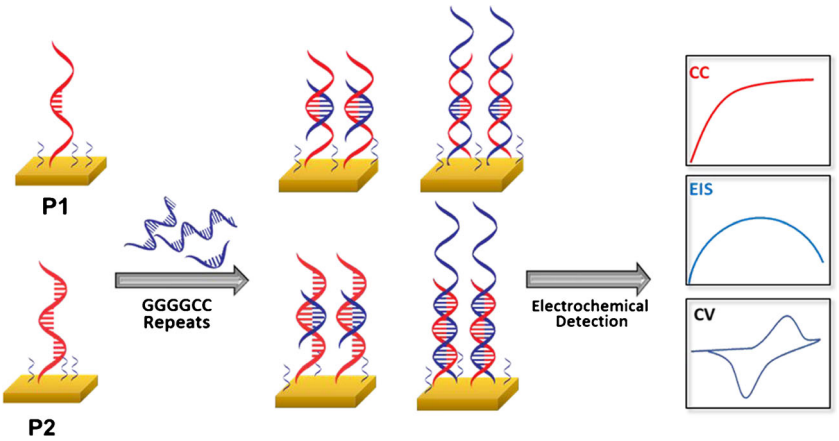

Scheme 1 Label-free detection of GGGGCC repeats of different lengths using 18-mer probes with single capturing repeat in the center (P1) and three tandem repeats (P2), and analyzed by chronocoulometry (CC), electrochemical impedance spectroscopy (EIS), and cyclic voltammetry (CV)

complete StemflexTM medium (ThermoFisher Scientific). Cells were grown in sterile incubators at 37 °C with 5% CO_2. RNA was extracted using the standard TRIzol extraction method. Briefly, the cell monolayer was rinsed with Dulbecco's Phosphate Buffered Saline (DPBS). The cells were then lysed directly in the culture dish by adding 1 ml of TRIzol reagent (ThermoFisher Scientific) to each well of a 6-well dish. Cell lysate was pipetted several times after a 3-min incubation. The solution was transferred to a 1.5 ml microfuge tube and 200 ml chloroform was added per 1 ml of TRIzol reagent. The sample was vortexed vigorously for 30 s and spun at 13,000×*g* for 5 min. After centrifugation, the aqueous phase was transferred (without disturbing the interphase/white precipitate) to a new tube. RNA was precipitated by adding one volume of isopropanol and incubating at – 20 °C for more than 1 h. After incubation, samples were spun at 13,000×*g* for 10 min to pellet RNA. RNA pellets were washed with 70% chilled ethanol and centrifuged at 13,000×*g* for 5 min. After brief air-drying, RNA was resuspended in RNA resuspension buffer (5 mM Tris, pH 7.0, 0.1 mM EDTA). RNA concentration was determined by UV-vis spectrophotometry (NanoDrop).

Probe immobilization and hybridization

First, the surface of gold working electrodes was regenerated by mechanical and electrochemical polishing. Briefly, gold disc electrodes of 2 mm diameter were polished with three different grain sizes of alumina powder (1, 0.3, and 0.05 μm) followed by 10-min sonication in DI water. Cyclic voltammetry was used for electrochemical cleaning of the mechanically polished electrodes by running 20 cycles in 0.5 M H_2SO_4 with a potential range of 0–1.5 V against an Ag/AgCl reference electrode and a platinum wire counter electrode. The gold oxide stripping peak of the last cycle was used to measure the roughness factor of the electrodes, which was kept at ≤ 1.2. In a separate set of experiments, freshly cleaned gold electrodes were incubated in 10 μM solutions of probe strands (P1 and P2) prepared in buffer (5× PBS pH = 7.4) as we previously reported [32]. The electrodes were capped with microcentrifuge tubes to prevent evaporation. Then the probe-modified electrodes were washed with buffer and further incubated in 1 mM mercaptohexanol for 30 min to block any unbound surface of the electrode and remove physically adsorbed DNA strands. After another washing step,

Table 1 Sequences of hexanucleotide DNA repeat expansion including probes, complementary sequences, and trinucleotide non-complementary sequences

Type	Sequence*	Repeat #	Nucleotide #	ID #
Probe	R-5′-ATT AGA ***CCC CGG*** AGA TTA-3′	1	18	P1
	R-5′-***CCC CGG CCC CGG CCC CGG***-3′	3	18	P2
Complementary HRE repeats	5′-CCG GGG-3′	1	6	C1
	5′-CCG GGG CCG GGG CCG GGG-3′	3	18	C3
	5′-CCG GGG CCG GGG CCG GGG CCG GGG CCG GGG CCG GGG-3′	6	36	C6
Non-complementary	5′-CTG CTG CTG CTG CTG CTG CTG CTG CTG-3′	9	27	NC

R = $HO(CH_2)_6$-S-S-$(CH_2)_6$-

*RNA repeat sequences are listed in supplementary information in Table S1

hybridization between the targets (C1, C3, and C6) and the surface-bound probe sequences (P1 and P2) was performed by pipetting 10 μL of 10 μM target sequence in buffer (5× PBS pH = 7.4) for 2 h at room temperature. Electrodes were washed with the buffer solution to remove any non-specifically bound oligonucleotides. For sensitivity studies, 5 μL samples containing 1–100 pmol of the longest DNA target (C6) were used with the surface-bound probes P1 or P2. For RNA samples containing 4–16 GGGGCC repeats, 5 μL of 5 μM samples were used for electrode preparation using the same protocol as described for the DNA samples. Huntington's disease (HD) samples were also diluted to final concentration of 54.54 ng·μL^{-1} and their 5 μL aliquot was used to challenge specificity of the P2 probes. For ALS sequence, 1000 ng·uL^{-1} of RNA was extracted from patient and the control samples while 5 μL aliquot of the samples was used for each P2 modified electrode to detect ALS biomarker sequence.

Electrochemical measurements

All electrochemical experiments were performed on a CHI 660E electrochemical instrument (CHI, Austin, TX) at room temperature in a three-electrode cell with the modified gold electrodes as the working electrode (with the geometric area of 0.0314 cm^2), platinum wire counter electrode, and Ag/AgCl reference electrode. In chronocoulometric studies, a potential step was applied to the DNA modified electrodes followed by measuring the resulting charge vs. (time)$^{1/2}$ under equilibrium conditions in the absence and presence of 5 μM $[Ru(NH_3)_6]^{3+}$ prepared in 10 mM Tri-ClO_4 (pH 7.4). The chronocoulometric measurements were carried out with the pulse period of 500 ms, pulse width of 600 mV (+ 150 to − 450 mV) and quiet time of 30 s. Deoxygenation of the solution was performed by purging the nitrogen gas through the buffer and redox marker solution for 30 min before measurement. Electrochemical impedance spectroscopy (EIS) was carried for single-stranded probes and double-stranded hexanucleotide GGGGCC expansion adducts using soluble redox probe, i.e., 1 mM $[Fe(CN)_6]^{3-/4-}$ prepared in 5× PBS (pH 7.4). The following parameters were used to run the EIS measurements: frequency range from 100 kHz to 1 Hz, an applied potential of 250 mV vs. Ag/AgCl, and AC voltage of 5 mV amplitude. For simulation, Z-view version 3.5d was used to fit the EIS data into Randle's equivalent circuit and to extract the values for charge transfer resistance (R_{CT}). Cyclic voltammetry measurements of the GGGGCC modified electrodes were also carried out in 1 mM $[Fe(CN)_6]^{3-/4-}$ using potential window − 0.4 to + 0.6 V with the scan rate of 50 mV/s.

Results and discussion

Surface density measurements

In this study, two DNA probes having the same length, but a different number of complementary repeats were employed to capture hexanucleotide GGGGCC repeats of different lengths in single-stranded DNA and RNA targets. Surface density of a DNA probe on an electrode surface plays a critical role in the sensitivity of affinity-based sensors. Chronocoulometry (CC) was used to calculate the number of single- and double-stranded DNA molecules on gold electrode surfaces as described previously [33, 34]. In particular, CC measures charge of an electrostatic label, Ru $(NH_3)_6^{3+}$, that binds with anionic DNA phosphate residue in 1:1 ratio, which in turn correlates with the number of strands on surface using a Cottrell equation (see supplementary information). Figure 1 a and b represent the typical CC curves for P1 and P2 probes along with their surface hybridized duplexes, respectively. Evidently, the surface densities were in similar order of magnitude as reported earlier for oligonucleotides of similar lengths [33]. However, Fig. 1c, d reveal a few interesting trends. P1 probe has significantly higher surface coverage ($8.8 \pm 0.7 \times 10^{12}$ molecules/cm^2), almost twice the P2 coverage ($4.9 \pm 0.4 \times 10^{12}$ molecules/cm^2), although both have the same number of nucleotides. This characteristic may be rationalized as an effect of the tandem repeats in P2, which are prone to intra-strand hybridization that perhaps increases the footprint of P2 leading to lower surface density. However, for both probes, the number of surface hybridized duplexes decreases with the number of repeats where the steep decline occurs from C1 to C3 coverage while a moderate decline from C3 to C6. The results show that hybridization efficiency (surface coverage of the duplexes) decreases with respect to length of the targets perhaps due to a subsequent increase in steric hindrance. In comparison to P1, the surface densities of P1-C3 and P1-C6 are ~ 10% and 5%, respectively. Whereas, the densities of P2-C3 and P2-C6 are ~ 20% and 10% respectively with respect to P2 density. This implies that capturing efficiency can be improved by introducing more hybridization sites in a probe.

Detection of GGGGCC repeats by electrochemical impedance spectroscopy

Electrochemical impedance spectroscopy (EIS) is a label-free biosensing approach [35–40], which not only detects base pair mismatches but also length mismatches between strands of a DNA duplex due to physical hindrance and charge accumulation at the electrode surface [41, 42]. Previous EIS-based detection of *CGG* and *TGG* repeats relied on specifically designed small molecules that can detect only single length of 10 repeat units. [25] However, small DNA probes have been found sensitive to varying lengths of

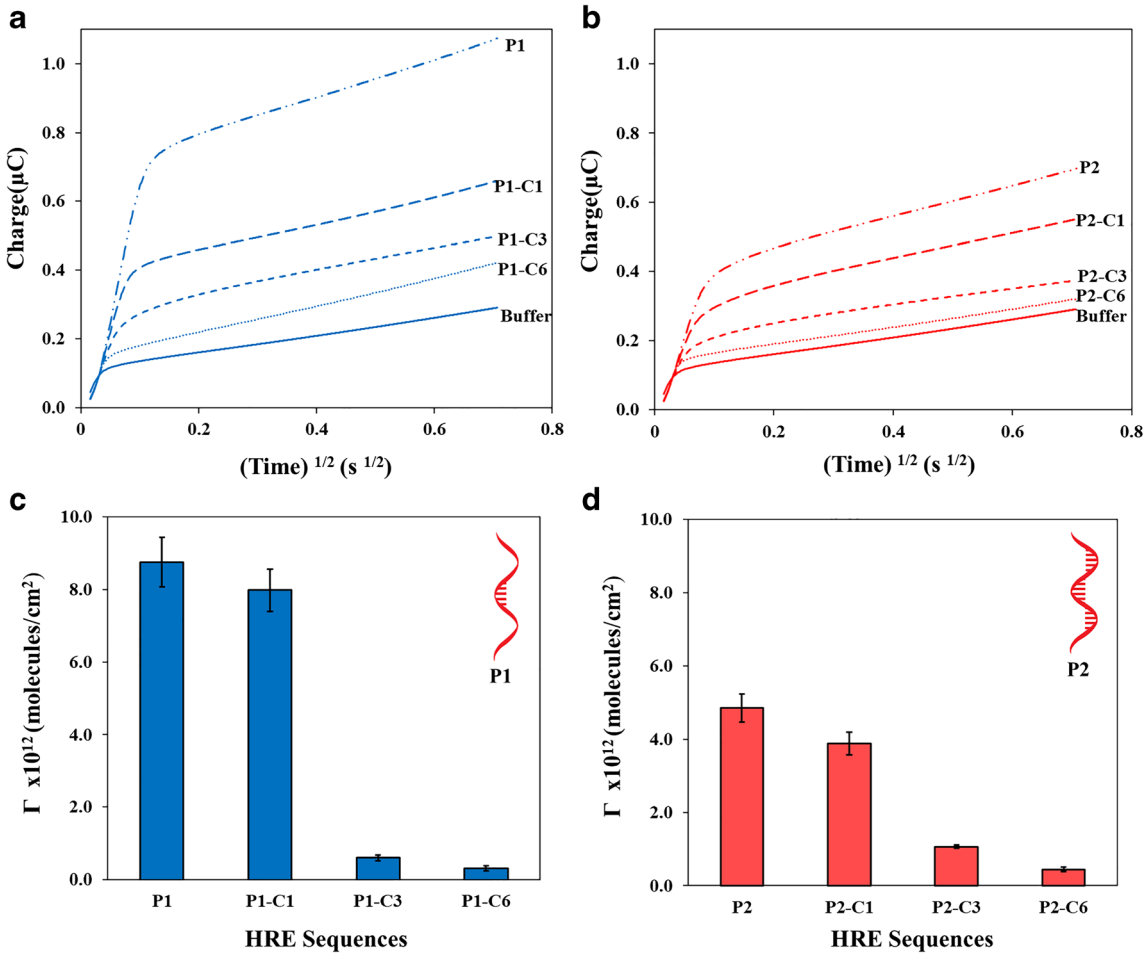

Fig. 1 **a**, **b** Representative chronocoulometry curves of P1 and P2 probes with 10 μM of target sequences C1, C3, and C6, before and after exposure to Ru $(NH_3)_6^{3+}$. **c**, **d** Bar graph shows the surface density of the hexanucleotide repeat probes (P1 and P2) and the surface hybridized adducts with complementary sequences having 1, 3, and 6 GGGGCC repeats (C1, C3, and C6). Error bars represent standard deviation for $N = 6$

target strands and transduced into unique R_{CT} signal [32, 41]. Here, the number of GGGGCC repeats was detected by simply monitoring the R_{CT} signal of the hybridization event with respect to length of repeats using small DNA probes P1 and P2. First, we tested the probes with single-stranded DNA targets having a small number of repeats, i.e., 1, 3, and 6 GGGGCC repeats. Figure 2 a and b represent the EIS plots for P1 and P2 accompanied by their hybridized duplexes with complementary and non-complementary targets. The Randle's equivalent circuit used to extract the R_{CT} is given in the supplementary information. Despite substantial difference in the surface densities, P1 and P2 showed similar R_{CT}, ~ 50 Ω·cm^2. This is attributed to the leaky nature of films comprising single-stranded DNA probes with flexible structure. Figure 2c represents the linear correlation between R_{CT} and the number of DNA repeats with P1 and P2. It is evident that despite decrease in the surface coverage of the duplexes with the number of GGGGCC repeats shown above, R_{CT} increases proportionally with both probes P1 and P2 but with different sensitivity. This can be rationalized due to the accumulation of negative charge by longer repeats that poses higher electrostatic repulsion to the negatively charged redox probe. This verifies that the accumulation of charge can be a significant contributor that may overcome the lack of target strands, thus, self-amplified R_{CT} signal can be obtained for longer repeats. The selectivity of the probes was also tested using a 27-mer non-complementary CTG trinucleotide repeat sequence. The R_{CT} values for CTG repeats are even lower than the single GGGGCC repeat, i.e., P1-NC (118 ± 9 Ω·cm^2) and P2-NC (158 ± 14 Ω·cm^2), which is due to the presence of intermittent base pair mismatch making the affinity between the probes and CTG repeats ineffective. Cyclic voltammetric measurements of the duplexes between the probes (P1 and P2) and the DNA targets (C1, C3, and C6) support the EIS results by showing the increase in overpotential with respect to target length (Fig. S1 in the supplementary information).

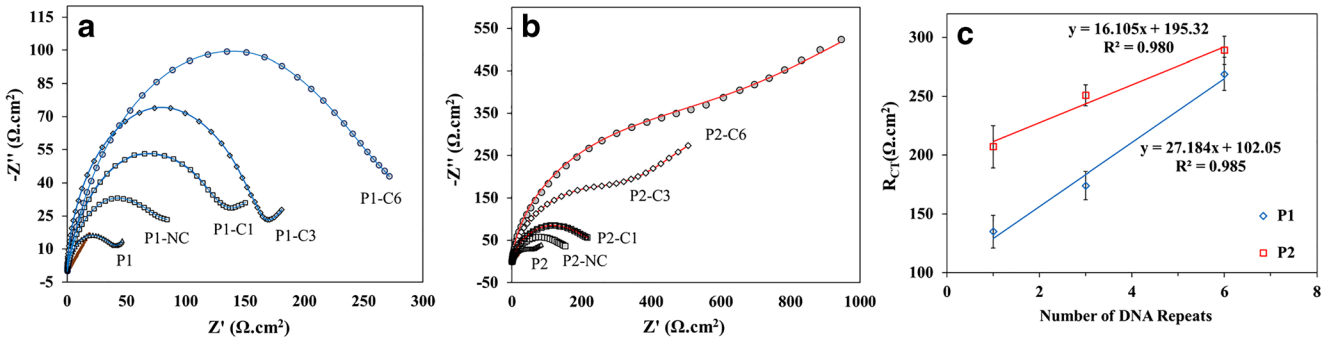

Fig. 2 **a**, **b** Nyquist form of EIS curves for P1 and P2 probes with 10 μM of target sequences C1, C3, C6, and non-complementary. **c** Curves showing correlation between the R_{CT} values extracted from the EIS for the DNA repeats. Error bars represent standard deviation for $N \geq 6$

Sensitivity performance of the probes

The quantitative performance of the new probes was assessed by evaluating a dilution series of the C6 complementary target to form P1-C6 and P2-C6 constructs on the surface. Figure 3 shows calibration curves for the experiments using 5 μL of 0–100 μM solutions of the C6 target sample, i.e., 0–100 pmol of absolute strands in the sample volume. The curves are best fit for 2nd order polynomial regression. The linear part of the calibration curves was fit into linear regression to calculate the limit of detection using LOD = 3 × (standard deviation of blank signal) ÷ sensitivity or slope of the curve. The absolute limits of detection were calculated as P1 = 6.8 pmol and P2 = 6.4 pmol, which is equal to 76.5 ng and 72.2 ng C6 target, respectively. The detection limit is three orders of magnitude better than the required sample amount for traditional Southern blotting method (~ 10 μg), however, slightly lower than other labeled electrochemical methods.

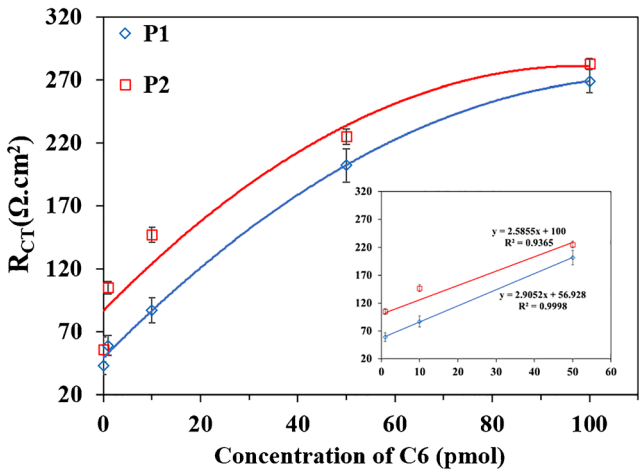

Fig. 3 Calibration curve obtained for P1-C6 and P2-C6 duplexes by EIS for 0–100 pmol concentrations of C6 repeat. Data was best fit in polynomial function. Error bars represent standard deviation for $N = 3$. Inset shows the linear part of the calibration curve

Since longer targets can self-amplify the R_{CT} signal due to higher amounts of negative charge, better LOD may be achievable for targets with more repeats.

Detecting GGGGCC repeats in RNA

Inspired by the fact that RNA copies are more accessible for hybridization because they are typically single-stranded, capturing efficiency of the probes was tested for a greater number of repeats (4–16 repeats) in RNA samples. The trend shown in Fig. 4 confirms the linear relationship between the R_{CT} and number of GGGGCC repeats in RNA where the tandem repeat probe 'P2' shows superior features than P1. First, amplified R_{CT} signal was observed for all GGGGCC repeats. Second, the slope of the curve verifies that the sensitivity of P2 for number of repeats is 3× higher than the P1 sensitivity.

Specificity of P2 probe and testing real samples

Huntington's disease (HD) is caused by 25+ expansion of CAG repeats in the HTT gene. The specificity of the P2 probe was examined against the CAG repeat using RNA strands with 72 repeat length. First, P2 was hybridized with HD (CAG-72) sequence in absence of GGGGCC repeats. Then, a competitive assay was performed using a 1:1 mixture containing R12 (GGGGCC-12 RNA) and the HD (CAG-72) RNA sequence. The R_{CT} response of the HD and R12+HD were compared with the complementary R12 only sequence in Fig. 5, which shows that the R_{CT} response of the R12+HD is same as the reference sequence 'R12.' In contrast, the HD response is substantially lower than the reference R12 signal. Therefore, it suggests that the response of R12+HD is due to the affinity between P2 and complementary GGGGCC repeats and there is a minimal interference of HD in presence of the 100% GC complementary sequence, which confirms the selectivity of P2 for GGGGCC repeats. Finally, cell extracted normal and

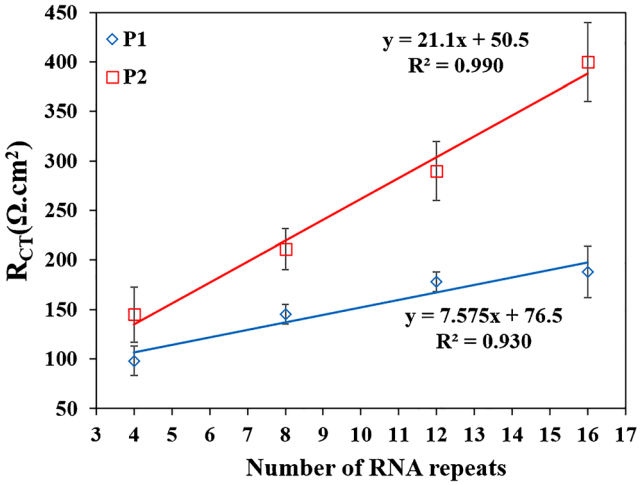

Fig. 4 Detection of GGGGCC repeats in RNA by EIS for 4–16 number of GGGGCC repeats of 5 μM RNA with measurement in triplicates

pathological GGGGCC repeats were detected using P2 probe using the protocol developed in this project. Figure 5 compares the R_{CT} ALS(−ve), which is control or normal repeat sequence less than 25 repeats, and ALS(+ve) which is expected to have hundreds of repeats. The R_{CT} response for the ALS(+ve) is higher and statistically distinguishable from the control, however not as high as the difference expected with these number of repeats. We suggest that certain signal amplification strategies such as addition of metal ions, as reported earlier [43], may be used to amplify the difference between the normal and abnormal repeat lengths and allow more precise sizing of repeat RNA in patient-derived samples.

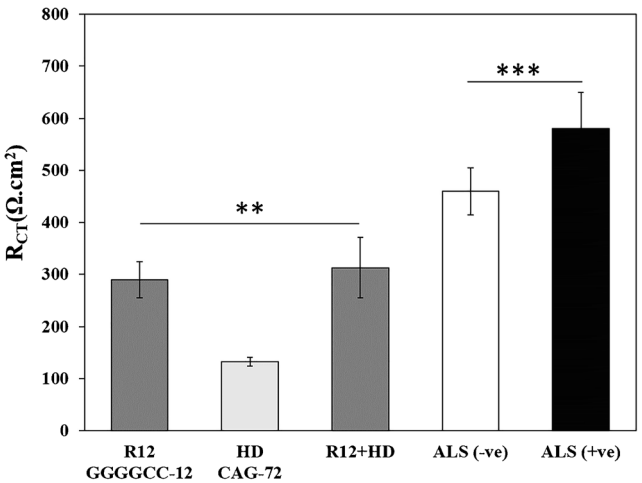

Fig. 5 **Selectivity test of P2 probe for GGGGCC repeats (R12) in presence of HD positive CAG sequence (72 repeats). ***Detection of GGGGCC repeats in patient-derived RNA samples where ALS(−ve) represent normal length of GGGGCC repeats and ALS(+ve) represents pathogenic length of GGGGCC repeats. Error bars represent standard deviation $N \geq 3$

Conclusion

Here, we have reported a novel strategy for label-free detection of hexanucleotide (GGGGCC) repeats associated with FTD and ALS using electrochemical impedance spectroscopy. The surface-bound probes transduced the hybridization event into charge transfer resistance (R_{CT}), which proportionately increased with the number of repeats in target despite the decrease in surface density of the hybridized duplexes with repeat length. The increase in R_{CT} response was observed despite a decrease in surface density with the increasing number of repeats in target sequences. The probe with three tandem repeats (P2) was found superior in many aspects. The calibration sensitivity of P2 was three times higher than P1 along with slightly better detection limit. Moreover, the selectivity of the probe was unaffected in the presence of patient-derived CAG repeat-containing sequence associated with Huntington's disease (HD). Moreover, the P2 probe is capable of distinguishing abnormal versus normal GGGGCC repeats in RNA extracted from patient-derived cells. We propose that the label-free approach demonstrated here may be applicable to the detection of repeat size for other types of repeat sequences using small probes with multiple complementary repeats. The amount of DNA that needs to be used for detecting the target DNA is significantly low compared to traditional Southern blotting methods.

Funding information M.H. Shamsi acknowledges SIUC startup funds for the research. L.M. Ellerby acknowledges R01 NS100529 grant. Funding to K.T.G. was provided by an Amyotrophic Lateral Sclerosis Research Program (ALSRP) grant from the US Department of Defense.

Compliance with ethical standards

Conflict of interest The authors declare that they have no conflict of interest.

References

1. The Genomes Project C, McVean GA e a. An integrated map of genetic variation from 1,092 human genomes. Nature. 2012;491:56.
2. Kozlowski P, de Mezer M, Krzyzosiak WJ. Trinucleotide repeats in human genome and exome. Nucleic Acids Res. 2010;38(12):4027–39.
3. Rohilla KJ, Gagnon KT. RNA biology of disease-associated microsatellite repeat expansions. Acta Neuropathol Commun. 2017;5(1):63.

4. Renton AE, Majounie E, Waite A, Simon-Sanchez J, Rollinson S, Gibbs JR, et al. A hexanucleotide repeat expansion in C9ORF72 is the cause of chromosome 9p21-linked ALS-FTD. Neuron. 2011;72(2):257–68.
5. DeJesus-Hernandez M, Mackenzie IR, Boeve BF, Boxer AL, Baker M, Rutherford NJ, et al. Expanded GGGGCC hexanucleotide repeat in noncoding region of C9ORF72 causes chromosome 9p-linked FTD and ALS. Neuron. 2011;72(2):245–56.
6. Buermans HPJ, den Dunnen JT. Next generation sequencing technology: advances and applications. Biochim Biophys Acta. 2014;1842(10):1932–41.
7. Orr HT, Zoghbi HY. Trinucleotide repeat disorders. Annu Rev Neurosci. 2007;30:575–621.
8. van Blitterswijk M, DeJesus-Hernandez M, Rademakers R. How do C9ORF72 repeat expansions cause amyotrophic lateral sclerosis and frontotemporal dementia: can we learn from other noncoding repeat expansion disorders? Curr Opin Neurol. 2012;25:689–700.
9. Zhao X, Usdin K. The repeat expansion diseases: the dark side of DNA repair. DNA Repair. 2015;32:96–105.
10. Chen LJ, Hadd A, Sah S, Filipovic-Sadic S, Krosting J, Sekinger E, et al. An information-rich CGG repeat primed PCR that detects the full range of fragile X expanded alleles and minimizes the need for southern blot analysis. J Mol Diagn. 2010;12(5):589–600.
11. Loomis EW, Eid JS, Peluso P, Yin J, Hickey L, Rank D, et al. Sequencing the unsequenceable: expanded CGG-repeat alleles of the fragile X gene. Genome Res. 2013;23(1):121–8.
12. Hubers A, Marroquin N, Schmoll B, Vielhaber S, Just M, Mayer B, et al. Polymerase chain reaction and southern blot-based analysis of the C9ORF72 hexanucleotide repeat in different motor neuron diseases. Neurobiol Aging. 2014;35(5):1214 e1–6.
13. Narzisi G, Schatz MC. The challenge of small-scale repeats for indel discovery. Front Bioeng Biotech. 2015;3:8.
14. Akimoto C, Volk AE, van Blitterswijk M, Van den Broeck M, Leblond CS, Lumbroso S, et al. A blinded international study on the reliability of genetic testing for GGGGCC-repeat expansions in C9orf72 reveals marked differences in results among 14 laboratories. J Med Genet. 2014;51(6):419–24.
15. Buchman VL, Cooper-Knock J, Connor-Robson N, Higginbottom A, Kirby J, Razinskaya OD, et al. Simultaneous and independent detection of C9ORF72 alleles with low and high number of GGGGCC repeats using an optimised protocol of Southern blot hybridisation. Mol Neurodegener. 2013;8(1):12.
16. Crook A, McEwen A, Fifita JA, Zhang K, Kwok JB, Halliday G, et al. The C9orf72 hexanucleotide repeat expansion presents a challenge for testing laboratories and genetic counseling. Amyotroph Lateral Scler Frontotemporal Degener. 2019;20(5–6):310–6.
17. Le Ber I. Genetics of frontotemporal lobar degeneration: an up-date and diagnosis algorithm. Rev Neurol. 2013;169(10):811–9.
18. Lunetta C, Lizio A, Melazzini MG, Maestri E, Sansone VA. Amyotrophic lateral sclerosis survival score (ALS-SS): a simple scoring system for early prediction of patient survival. Amyotroph Lateral Scler Frontotemporal Degener. 2015;17(1–2):93–100.
19. Park J-Y, Park S-M. DNA hybridization sensors based on electrochemical impedance spectroscopy as a detection tool. Sensors. 2009;9(12):9513.
20. Fojta M, Havran L, Vojtiskova M, Palecek E. Electrochemical detection of DNA triplet repeat expansion. J Am Chem Soc. 2004;126(21):6532–3.
21. Liu YL, Li J, Chang G, Zhu RZ, He HP, Zhang XH, et al. A novel electrochemical method based on screen-printed electrodes and magnetic beads for detection of trinucleotide repeat sequence d(CAG)(n). New J Chem. 2018;42(12):9757–63.
22. Zhu XQ, Li J, Lv HH, He HP, Liu H, Zhang XH, et al. Synthesis and characterization of a bifunctional nanoprobe for CGG trinucleotide repeat detection. RSC Adv. 2017;7(57):36124–31.
23. Li J, Liu Y, Zhu X, Chang G, He H, Zhang X, et al. A novel electrochemical biosensor based on a double-signal technique for d(CAG)n trinucleotide repeats. ACS Appl Mater Interfaces. 2017;9(50):44231–40.
24. He H, Xia J, Peng X, Chang G, Zhang X, Wang Y, et al. Facile electrochemical biosensor based on a new bifunctional probe for label-free detection of CGG trinucleotide repeat. Biosens Bioelectron. 2013;49:282–9.
25. He H, Peng X, Huang M, Chang G, Zhang X, Wang S. An electrochemical impedance sensor based on a small molecule modified Au electrode for the recognition of a trinucleotide repeat. Analyst. 2014;139(21):5482–7.
26. Fojta M, Havran L, Kizek R, Billova S, Palecek E. Multiply osmium-labeled reporter probes for electrochemical DNA hybridization assays: detection of trinucleotide repeats. Biosens Bioelectron. 2004;20(5):985–94.
27. Miroslav F, Petra B, Kateřina C, Petr P. A single-surface electrochemical biosensor for the detection of DNA triplet repeat expansion. Electroanalysis. 2006;18(2):141–51.
28. Yang IV, Thorp HH. Kinetics of metal-mediated one-electron oxidation of guanine in polymeric DNA and in oligonucleotides containing trinucleotide repeat sequences. Inorg Chem. 2000;39(21):4969–76.
29. Yang IV, Thorp HH. Modification of indium tin oxide electrodes with repeat polynucleotides: electrochemical detection of trinucleotide repeat expansion. Anal Chem. 2001;73(21):5316–22.
30. Kartje ZJ, Barkau CL, Rohilla KJ, Ageely EA, Gagnon KT. Chimeric guides probe and enhance Cas9 biochemical activity. Biochemistry. 2018;57(21):3027–31.
31. An MC, Zhang N, Scott G, Montoro D, Wittkop T, Mooney S, et al. Genetic correction of Huntington's disease phenotypes in induced pluripotent stem cells. Cell Stem Cell. 2012;11(2):253–63.
32. Shamsi MH, Kraatz H-B. The effects of oligonucleotide overhangs on the surface hybridization in DNA films: an impedance study. Analyst. 2011;136(15):3107–12.
33. Steel AB, Herne TM, Tarlov MJ. Electrochemical quantitation of DNA immobilized on gold. Anal Chem. 1998;70(22):4670–7.
34. Ge B, Huang Y-C, Sen D, Yu H-Z. Electrochemical investigation of DNA-modified surfaces: from quantitation methods to experimental conditions. J Electroanal Chem. 2007;602(2):156–62.
35. Capaldo P, Alfarano SR, Ianeselli L, Zilio SD, Bosco A, Parisse P, et al. Circulating disease biomarker detection in complex matrices: real-time, in situ measurements of DNA/miRNA hybridization via electrochemical impedance spectroscopy. ACS Sensors. 2016;1(8):1003–10.
36. Bertok T, Lorencova L, Chocholova E, Jane E, Vikartovska A, Kasak P, et al. Electrochemical impedance spectroscopy based biosensors: mechanistic principles, analytical examples and challenges towards commercialization for assays of protein cancer biomarkers. ChemElectroChem. 2019;6(4):989–1003.
37. Yang J, Jiao K, Yang T. A DNA electrochemical sensor prepared by electrodepositing zirconia on composite films of single-walled carbon nanotubes and poly(2,6-pyridinedicarboxylic acid), and its application to detection of the PAT gene fragment. Anal Bioanal Chem. 2007;389(3):913–21.
38. Kerman K, Morita Y, Takamura Y, Tamiya E. Escherichia coli single-strand binding protein–DNA interactions on carbon nanotube-modified electrodes from a label-free electrochemical hybridization sensor. Anal Bioanal Chem. 2005;381(6):1114–21.
39. Lisdat F, Schäfer D. The use of electrochemical impedance spectroscopy for biosensing. Anal Bioanal Chem. 2008;391(5):1555.
40. Ding S, Mosher C, Lee XY, Das SR, Cargill AA, Tang X, et al. Rapid and label-free detection of interferon gamma via an electrochemical aptasensor comprising a ternary surface monolayer on a gold interdigitated electrode array. ACS Sensors. 2017;2(2):210–7.

41. Riedel M, Kartchemnik J, Schoning MJ, Lisdat F. Impedimetric DNA detection-steps forward to sensorial application. Anal Chem. 2014;86(15):7867–74.
42. Shamsi MH, Kraatz HB. Probing nucleobase mismatch variations by electrochemical techniques: exploring the effects of position and nature of the single-nucleotide mismatch. Analyst. 2010;135(9): 2280–5.
43. Alam MN, Shamsi MH, Kraatz HB. Scanning positional variations in single-nucleotide polymorphism of DNA: an electrochemical study. Analyst. 2012;137(18):4220–5.